MODELLING OF MULTI-LAYERED QUANTUM WELL PHOTOVOLTAIC CELLS

Vladimir IANCU[1], Mihai Răzvan MITROI[2], Laurențiu FARA[3]

Lucrarea prezintă modelarea celulelor fotovoltaice multistrat cu gropi cuantice. Confinarea cuantică a unui semiconductor introduce noi nivele de energie localizate în banda interzisă, ca şi nivele rezonante localizate în benzile de conducţie şi valenţă. Aceste nivele permit o absorbţie suplimentară în domeniile vizibil şi infraroşu apropiat. Eficienţa cuantică internă pentru absorbţia suplimentară a fost calculată în aproximaţia gropii de potenţial rectangulară infinită.S-au sugerat îmbunătăţiri optice ale celulei, pentru a mări absorbţia suplimentară.

The present paper discusses the modelling of the multi-layered quantum well photovoltaic cells. The quantum confinement of a semiconductor induces new energy levels, located in the band gap, as well as resonant levels located in the conduction and valence bands. These levels allow supplementary absorption in visible and near infrared range. The internal quantum efficiency for the supplementary absorption was calculated within the infinite rectangular quantum well approximation. Optical improvements of the cell were suggested, in order to improve the supplementary absorption.

Keywords: Photovoltaic cells; Quantum wells; Multi-layered structures

1. Introduction

The "quantum well" photovoltaic cells were first proposed in 1990 [1], based on the idea that the use of the quantum wells could improve the photovoltaic cells by extending their spectral response, as well as by increasing the photocurrent. One year later, this idea was experimentally proved by using a $GaAs/Al_xGa_{1-x}As$ multi-layered structure [2]. From then on, the use of the multi-layered photovoltaic (MLPV) cells became one of the most used approaches for a high efficiency PV cell. Generally, such cells are p-i-n type diodes, with the intrinsic region formed by a multilayered structure [3 - 11]. Most of these cells have layers of tens or even hundreds of nanometer thickness, so that the quantum

[1] Lecturer, Physics Chair II, Applied Sciences Faculty, University POLITEHNICA of Bucharest, Romania; e-mail: codas@physics.pub.ro
[2] Reader, Physics Chair II, Applied Sciences Faculty, University POLITEHNICA of Bucharest, Romania
[3] Prof., Physics Chair II, Applied Sciences Faculty, University POLITEHNICA of Bucharest, Romania

effects are reduced; nevertheless they are also called in some texts "quantum well" PV cells. However, MLPV cells with real quantum sizes (multi-layered quantum well photovoltaic – MLQWPV) are also studied [10, 11].

An analysis of the quantum effects proves that the quantum size appears under about 20 interatomic distances (e.g. about 5 nm), where the band structure is replaced by an energy level structure and the momentum conservation law is no longer valid [12].

The true quantum well photovoltaic cells use the special advantages of the low dimensional systems, where at least one size is at quantum scale. This leads to two important contributions. The first contribution is a strong quantum confinement (QC) effect. Indeed, at this size, it was proved that the material nature role is secondary with respect to the QC [13, 14]. The second contribution is the increased role of the surface/interface. The area/volume ratio is of the order of $1/d$, where d is the minimum size, so that, at quantum sizes, this ratio is greater than 2×10^8 m^{-1}. Then, the cells are classified with respect to their dimensionality in 2D, 1D, 0D and fractals. The MLPV (and the multi-layered quantum well photovoltaic – MLQWPV) cells are 2D. In literature, they are divided in multiple quantum wells (MQW) and superlattice (SL) systems [10], the difference being based on the barrier layer thickness [10]. However, this interpretation is not correct. The SL structures replace the resonant levels from the conduction and valence bands of the "quantum wells" with resonant bands. This is not only correlated with the barrier thickness, but also with the total number of layers, for reasons similar with those that define the quantum size [12]. In the following, only MQW structures will be considered.

The aim of this paper is to model MLQWPV cells in order to find out how to improve them. Section 2 deals with the QC effects. Section 3 calculates the internal quantum efficiency of a layer. Section 4 discusses the optical improvements necessary for these cells. The last Section summarizes the obtained results.

2. QC effects

As it was stated in Section 1, the MLQWPV cells have a p-i-n structure, with a multi-layered i region (e.g. $GaAs/Al_xGa_{1-x}As$). It is well known that the band gap difference between the layers acts like a quantum well and induces the appearance of resonant levels in both the conduction and valence bands (MQW structure). These levels improve the absorption and therefore increase the cell efficiency. If the number of layers is big enough and if they are thin enough, the resonant levels are replaced with resonant bands (SL structure). An example of both structures, under an external bias V, is presented in Fig. 1 (based on Fig. 2, Ref. 14). E_w, t_w and E_b, t_b are the gaps and thicknesses of the quantum well and

barrier layers, respectively. For MLQWPV cells, both t_w and t_b are of the order of 5 – 10 nm.

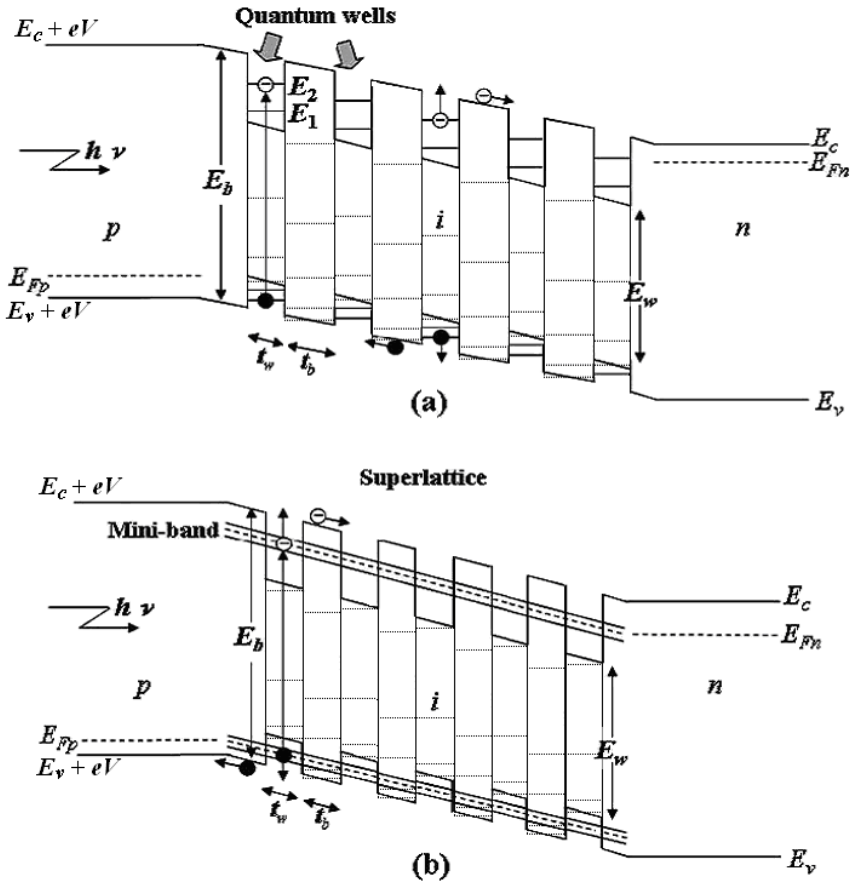

Fig. 1. (a) MQW and (b) SL p-i-n structures under applied bias V. Solid lines - the resonant levels (a) and bands (b); dotted lines - the QC levels.

Several studies [13 - 15] proved that the main quantum confinement (QC) effect consists in the introduction of QC levels in the band gap. Indeed, the surface/interface of a low dimensional system acts like the wall of a quantum well. The analysis of different shapes proved that the rectangular quantum well is good enough for the description of the QC effects.

There are two more problems to analyze. The first one is the depth of the potential well. It was proved that, for rectangular quantum wells, deeper than 2 eV and larger than 1 nm, the differences between the first three levels in the finite well and the infinite well with the same width is less than 2.5 % [13], so that the

use of the infinite rectangular quantum well (IRQW) approximation does not exceed the experimental errors. As the relative error is proportional with $t\sqrt{U}$, where U is the potential well depth, it results that the IRQW approximation does not lead to errors greater than about 5 % for any known MQW or SL structure (e.g. for t = 10 nm, it is enough to have $U > 0.02$ eV).

The second problem is the location of these supplementary energy levels. As at absolute zero temperature the maximum energy of an electron in a semiconductor corresponds with the top of the valence band, the fundamental quantum confinement level should be located at this energy value. This means that the QC levels must be located in the band gap.

The electron energy has the expression:

$$E = \varepsilon_{n\vec{k}} + \frac{\pi^2\hbar^2}{2m_t^* t^2} p^2 = \left(\varepsilon_{n\vec{k}} + \frac{\pi^2\hbar^2}{2m_t^* t^2} \right) + \frac{\pi^2\hbar^2}{2m_t^* t^2} \left(p^2 - 1 \right) \equiv \varepsilon_{n\vec{k}}^{(s)} + E_{p-1}, \qquad (1)$$

where $\varepsilon_{n\vec{k}}^{(s)}$ is the shifted 2D band energy, $E_{p\text{-}1}$ is the QC level energy ($E_0 \equiv 0$), m_t^* is the transversal effective electron mass, and t the layer thickness. These QC levels induce supplementary absorption in the visible and near infrared range. It is important to remark that these levels appear in both narrow and wide gap layers. At the same time, one can see from Fig. 1 that, at convenient bias value, some levels from the consecutive quantum well and barrier layers have practically the same energy value (differences under k_BT). This strongly increases the tunnelling rate through the junction.

3. Optical absorption

The band-to-band absorption will not be discussed in this paper, which is focused only on the absorption induced by the resonant levels and by the QC levels from the gap. The absorption rate is proportional with the square modulus of the matrix element of the transition Hamiltonian between the initial and final state:

$$R_\lambda = \frac{2\pi}{\hbar} \left| H_{fi} \right|^2 \delta\left(\Delta E - \frac{hc}{\lambda} \right). \qquad (2)$$

If one takes into account only the electric dipole transition (as it is the most probable) and if one uses the IRQW approximation, the matrix element becomes:

$$H_{fi} = -\frac{2}{t} e \int_0^t \vec{E} \cdot \vec{r} \sin \frac{p_f \pi z}{t} \sin \frac{p_i \pi z}{t} dz \,, \tag{3}$$

where p_i, p_f are natural non-zero numbers (the elementary charge e is considered positive throughout this paper).

The calculations are performed for $\vec{E}$ parallel with or perpendicular on the layer, considering a square cell with the lateral size L. In the first case, the position vector does not depend on z and its mean value is $L/2$. Then, the matrix element equals $eE_{x,y} \cdot L/2$ if and only if $p_f = p_i$. This case describes the pair generation by means of transitions between resonant states from the valence and conduction bands. In the second case, the matrix element is $eE_{x,y} \cdot t/2$ if $p_f = p_i$ (transitions between resonant states) and

$$H_{fi} = \frac{eE_z t}{\pi^2} \left[\frac{1-(-1)^{p_f - p_i}}{(p_f - p_i)^2} - \frac{1-(-1)^{p_f + p_i}}{(p_f + p_i)^2} \right] \tag{4}$$

(transitions between QC levels). This term is different from zero if and only if $p_f - p_i = 2p - 1$. Usually, the absorption transitions between QC levels start from $p_i = 1$ (top of the valence band, as the valence band acts as an electron reservoir). Taking into account the Snell-Descartes rule, one can express E_z for different polarizations. For polarization parallel with the incidence plane, $E_{\|z} = E_{\|} \sin\theta / \sqrt{\varepsilon_r} = \sqrt{E_{\|}^2 - E_{\|x,y}^2}$ (θ is the external incidence angle), while for polarization perpendicular on the incidence plane $E_{\perp z} = 0$. As the solar light is not polarized, $E_{\|} = E_{\perp} = E/\sqrt{2}$.

Then, the absorption rate is

$$R_\lambda = \frac{\pi e^2 \langle E^2 \rangle}{\hbar} \left[L^2 \left(1 - \frac{\sin^2\theta}{4\varepsilon_w} \right) + t_w^2 \frac{\sin^2\theta}{4\varepsilon_w} \right] \delta\left(\Delta E - \frac{hc}{\lambda} \right) \tag{5}$$

for transitions between resonant symmetric levels in the quantum well. Here ε_w is the relative permittivity of the quantum well layers (see Fig. 1) and $\Delta E = hc/\lambda = E_w + \pi^2 \hbar^2 / 2 m_w^* t_w^2$, where E_w is the corresponding gap and $m_w^* = \left(1/m_{ew}^* + 1/m_{hw}^* \right)^{-1}$ is the excitonic effective mass.

For transitions between the top of the valence band and the QC levels, the absorption rate becomes

$$R_{\lambda_p} = \frac{512e^2 t_{w,b}^2 \left\langle E^2 \right\rangle}{\pi^3 \hbar \varepsilon_{w,b}} \cdot \frac{p^2 \sin^2\theta}{\left(4p^2 - 1\right)^4} \delta\left(\Delta E_p - \frac{hc}{\lambda_p}\right), \tag{6}$$

where $\Delta E_p = hc/\lambda_p = \left[\left(\pi^2\hbar^2\right)/\left(2m_{tw,b}^* t_{w,b}^2\right)\right] \cdot \left(4p^2 - 1\right)$ and the constants correspond to the considered layer – either quantum well or barrier.

The Einstein absorption coefficient for a layer becomes

$$B_\lambda = \frac{\pi e^2 L^2}{\hbar^2 \varepsilon_0 \varepsilon_w} \left[\left(1 - \frac{\sin^2\theta}{4\varepsilon_w}\right) + \frac{t_w^2}{L^2} \frac{\sin^2\theta}{4\varepsilon_w}\right] \tag{7}$$

for transitions between resonant symmetric levels in the quantum well and

$$B_{\lambda_p} = \frac{512e^2 L^2}{\pi^3 \hbar^2 \varepsilon_0 \varepsilon_{w,b}^2} \cdot \frac{t_{w,b}^2}{L^2} \frac{p^2 \sin^2\theta}{\left(4p^2 - 1\right)^4} \tag{8}$$

for transitions between the top of the valence band and the QC levels.

The internal quantum efficiency is related to the Einstein absorption coefficient by the relation

$$\eta = \frac{8\pi\hbar}{cL^2} B, \tag{9}$$

so that one obtains

$$\eta_\lambda = \frac{8\pi^2 e^2}{c\hbar \varepsilon_0 \varepsilon_w} \left[\left(1 - \frac{\sin^2\theta}{4\varepsilon_w}\right) + \frac{t_w^2}{L^2} \frac{\sin^2\theta}{4\varepsilon_w}\right] \tag{10}$$

for the transitions between resonant symmetric levels in the quantum well and

$$\eta_{\lambda_p} = \frac{4096e^2}{\pi^2 c\hbar\varepsilon_0\varepsilon_{w,b}^2}\cdot\frac{t_{w,b}^2}{L^2}\frac{p^2\sin^2\theta}{\left(4p^2-1\right)^4} \tag{11}$$

for the transitions between the top of the valence band and the QC levels. One can observe that the quantum efficiency for the transitions between the top of the valence band and the QC levels is several orders of magnitude smaller than the one for transitions between resonant symmetric levels in the quantum well.

4. Optical improvements

From Eqs. (6, 8, 11) it results that the QC levels are active only for non-normal incidence. This insignificantly reduces the absorption on resonant levels. On the other hand, the absorption in the gap also improves the transport. Indeed, as the absorption excites carriers in the gap of each layer, even a small absorption significantly increases the photocurrent (by photoassisted tunneling). In order to ensure a non-normal incidence for any (visible) position of the Sun, one could place a refractive grating made from parallel prisms on the front surface of the cell (see Fig. 2), the prism edges being oriented on East-West direction.

If we quote the prism angle with α, the prism refraction index with n and the incidence angle (the angle of the light beam with the normal to the layer surfaces) with θ (as previous), then, in Eqs. (5 - 8, 10, 11), $\sin^2\theta$ must be replaced with $\sin^2\theta + \delta\sin^2\theta$, where

$$\delta\sin^2\theta = \frac{1+\cos\alpha}{2}\left\{n_p^2 - \cos\alpha - (1-\cos\alpha)\sin^2\theta - \sqrt{(1-\cos\alpha)\left[2n_p^2 - 1 - \cos\alpha - (1-\cos\alpha)\sin^2\theta\right]}\right\} \neq 0. \tag{12}$$

As the prism refraction index is always smaller than the semiconductor refraction indices, there is no risk of internal total reflection in any layer.

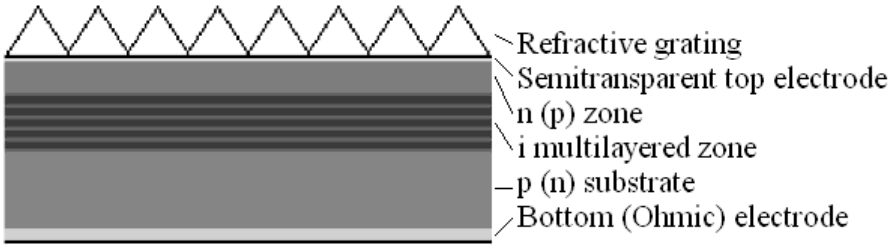

Fig. 2. Schematics of a p-i-n MLQWPV cell with refractive grating.

The results are presented in Figs. 3 and 4. The internal quantum efficiencies are computed with the relations (10 – 12). We have considered the $GaAs/Al_xGa_{1-x}As$ structure, with $L = 1$ cm, $t_w = t_b = 10$ nm, $n_p = 1.5$, $\alpha = \pi/2$, and $p = 2$ (for the excited QC). The values for the relative permittivity were taken from the literature [16].

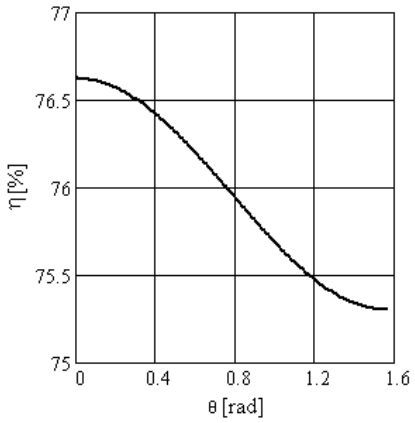

Fig. 3. Internal quantum efficiency for transitions between resonant symmetric levels in the GaAs quantum well versus the incidence angle.

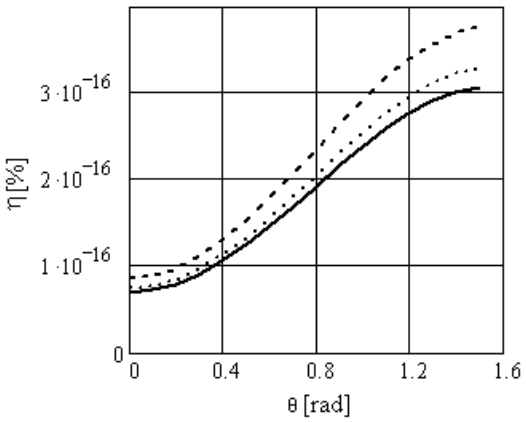

Fig. 4. Internal quantum efficiency for transitions between the top of the valence band and the QC levels in $Al_xGa_{1-x}As$ versus the incidence angle, for quantum wells (x = 0 – full line) and quantum barriers (x = 0.2 – dotted line and x = 0.4 – dashed line).

One can observe that the internal quantum efficiency for the transitions between the top of the valence band and the QC levels is seventeen orders of

magnitude smaller than the one for transitions between resonant symmetric levels in the quantum well, so that apparently it could be neglected. However, the excitation of even a few carriers in the band gap, on QC levels that are practically equal between the consecutive layers (due to a conveniently chosen bias), leads to a photoassisted tunnelling and significantly increases the photocurrent.

5. Conclusions

It was shown that the QC introduces energy levels not only in the conduction and valence bands (resonant levels), but also in the band gaps (QC levels). The corresponding energy values can be estimated from IRQW approximation with a good precision. On this basis, the internal quantum efficiency of the absorption for both transitions between resonant symmetric levels in the quantum gap, and transitions between QC levels and the top of the valence bands, was calculated. A refractive grating was proposed in order to ensure good absorption conditions at any Sun position. From the above discussion it results that the MLQWPV cells present several advantages on the classical PV cells: increased efficiency, wider spectral response, increased controllability. Therefore, in spite of the high accuracy needed for their fabrication, the MLQWPV cells represent one of the best solutions of the solar energy problem.

R E F E R E N C E S

[1] *K. W. J. Barnham and G. Duggan*, A new approach to high-efficiency multi-band-gap solar cells, J. Appl. Phys., **vol. 67**, 1990, pp. 3490-3493.

[2] *K. W. J. Barnham, B. Braun, J. Nelson, M. Paxman*, Short-circuit current and energy efficiency enhancement in a low-dimensional structure photovoltaic device**,** Appl. Phys. Lett., **vol. 59**, 1991, pp. 135-137.

[3] *M. Paxman, J. Nelson, B. Braun, J. Connolly, K. W. J. Barnham, C. T. Foxon, and J. S. Roberts*, Modeling the spectral response of the quantum well solar cell, J. Appl. Phys., **vol. 74**, 1993, pp.614-621.

[4] *N. G. Anderson*, Ideal theory of quantum well solar cells, J. Appl. Phys., **vol. 78**, 1995 pp. 1850-1861.

[5] *O. Y. Raisky, W. B. Wang, R. R. Alfano, C. L. Reynolds Jr., D. V. Stampone, and M. W. Focht*, Resonant enhancement of the photocurrent in multiple-quantum-well photovoltaic devices, Appl. Phys. Lett., **vol. 74**, 1999, pp. 129-131.

[6] *M. A. Green*, Prospects for photovoltaic efficiency enhancement using low-dimensional structures, Nanotechnology, **vol. 11**, 2000, pp. 401-405.

[7] *K. W. J. Barnham, I. Ballard, J. P. Connolly, N. J. Ekins-Daukes, B. G. Kluftinger, J. Nelson, C. Rohr*, Quantum well solar cells, Physica E, **vol. 14**, 2002, pp. 27-36.

[8] *N. G. Anderson*, On quantum well solar cell efficiencies, Physica E, **vol. 14**, 2002, pp.126-131.

[9] *Y. Sato, K. Yamagishi, and M. Yamashita*, Multilayer Structure Photovoltaic Cells, Opt. Rev., **vol. 12**, 2005, pp. 324-327.

[10] *S. Y. Myong*, Recent progress in inorganic solar cells using quantum structures, Recent Patents Nanotechnol., **vol. 1**, 2007, pp. 67-73.

[11] *Z. R. Hong, B. Maennig, R. Lessmann, M. Pfeiffer, K. Leo, and P. Simon*, Improved efficiency of zinc phthalocyanine/C60 based photovoltaic cells via nanoscale interface modification, Appl. Phys. Lett., **vol. 90**, 2007, 230505 (pp. 1-3).

[12] *J. Heitmann, F. Müller, L. X. Yi, M. Zacharias, D. Kovalev, and F. Eichhorn*, Excitons in Si nanocrystals: Confinement and migration effects, Phys. Rev. B, **vol. 69**, 2004, 195309 (pp. 1-7).

[13] *V. Iancu and M. L. Ciurea*, Quantum confinement model for electric transport phenomena in fresh and stored photoluminescent porous silicon films, Solid State Electron., **vol. 42**, 1998, pp. 1893-1896.

[14] *V. Iancu, M. L. Ciurea, and I. Stavarache*, Quantum confinement modeling of electrical and optical processes in nanocrystalline silicon, J. Optoelectron. Adv. Mater., **vol. 8**, 2006, pp. 2156-2160.

[15] *O. Pana, L. M. Giurgiu, Al. Darabont, V. Iancu, M. L. Ciurea, M. N. Grecu, and A. Boț*, Core-shell effects in granular perovskite manganites, J. Phys. Chem. Solids, **vol. 67**, 2006 pp. 624–627.

[16] *S. Adachi*, GaAs, AlAs, and $Al_xGa_{1-x}As$ Material parameters for use in research and device applications**,** J. Appl. Phys., **vol. 58**, 1985, pp. R1-R29.